JCTC Journal of Chemical Theory and Computation

Article

pubs.acs.org/JCTC

Benchmark Structures and Harmonic Vibrational Frequencies Near the CCSD(T) Complete Basis Set Limit for Small Water Clusters: $(H_2O)_n$ = 2, 3, 4, 5, 6

J. Coleman Howard and Gregory S. Tschumper*

Department of Chemistry and Biochemistry, University of Mississippi, University, Mississippi 38677−1848, United States

Supporting Information

ABSTRACT: A series of $(H_2O)_n$ clusters ranging from the dimer to the hexamer have been characterized with the CCSD(T) and the 2-body:Many-body CCSD(T):MP2 methods near the complete basis set (CBS) limit to generate benchmark-quality optimized structures and harmonic vibrational frequencies for these important systems. Quadruple-ζ correlation-consistent basis sets that augment the O atoms with diffuse functions have been employed in the analytic computation of harmonic vibrational frequencies for the global minima of the dimer, trimer, tetramer, and pentamer as well as the ring, book, cage, and prism isomers of the hexamer. Prior calibration [*J. Chem. Phys.* **2013**, *139*, 184113 and *J. Chem. Theory Comput.* **2014**, *10*, 5426] suggests that harmonic frequencies computed with this approach will lie within a few cm^{-1} of the canonical CCSD(T) CBS limit. These data are used as reference values to gauge the performance of harmonic frequencies obtained with other ab initio methods (e.g., LCCSD(T) and MP2) and water potentials (e.g., TTM3-F and WHBB). This comparison reveals that it is far more challenging to converge harmonic vibrational frequencies for the bound OH stretching modes in these $(H_2O)_n$ clusters to the CCSD(T) CBS limit than the free OH stretches, the n intramonomer HOH bending modes and even the $6n - 6$ intermonomer modes. Deviations associated with the bound OH stretching harmonic frequencies increase rapidly with the size of the cluster for all methods and potentials examined, as do the corresponding frequency shifts relative to the monomer OH stretches.

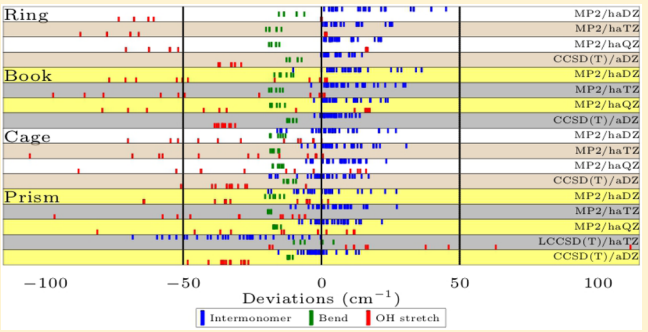

1. INTRODUCTION

Hydrogen bonding plays critical roles in a variety of biological and environmental phenomena.[1−6] As the noncovalent interaction that binds together H_2O molecules, hydrogen bonding is ultimately responsible for the unique properties of water. Obtaining reliable theoretical descriptions of the simplest water clusters is an essential step to understanding the complex hydrogen-bonding dynamics in liquid water.[7] To this end, ab initio quantum mechanical (QM) wave function methods have provided valuable insight into the structures and energetics of small water clusters.[8]

The water dimer is the smallest water cluster and has long served as a model for hydrogen-bonding interactions since the first ab initio investigations into $(H_2O)_2$.[9−18] As a small model system, the $(H_2O)_2$ global minimum has been the focus of benchmark electronic structure calculations,[19−21] at levels of electron correlation typically too demanding for larger chemical systems. An accurate description of $(H_2O)_2$ is crucial in the development of water potentials, as pairwise interactions are the dominant stabilizing force in larger clusters.[13,22−31] However, larger clusters offer insight into an important phenomenon missing in the dimer, hydrogen-bonding cooperativity.[31]

The global minima for $(H_2O)_n$ (n = 3−5) are characterized by cyclic homodromic hydrogen-bonding networks (i.e., each H_2O accepts and donates one hydrogen bond). Energetics of these small, cyclic minima (see Figure 1) have been examined at correlated levels in detail.[25,32−46] The efforts of Xantheas and coworkers[27,47−50] have been particularly important in establishing benchmark energetics and basis set convergence patterns in these systems. Second-order Møller−Plesset perturbation theory (MP2)[51] within the "frozen-core" approximation is sufficient for calculating high-accuracy energetics for the lowest energy configurations of these small cyclic clusters, as the effect of correlating the core electrons is of the same small magnitude but opposite sign of including higher-order dynamical electron correlation in the valence space.[41,52] Infrared vibrational spectra of the neutral $(H_2O)_m$ (m = 3−5) cyclic minima have been measured in the gas phase[53,54] in helium droplets[55,56] and also in solid matrix environments.[57,58]

When the hydrogen-bonding topology ceases to follow the homodromic pattern seen for water trimer, tetramer, and pentamer minima, MP2 is no longer sufficient for establishing benchmark-quality ab initio energies because the higher-order correlation effects can be appreciable and quite different for each type of network.[59] The water hexamer represents an important

Received: March 8, 2015

DOI: 10.1021/acs.jctc.5b00225
J. Chem. Theory Comput. XXXX, XXX, XXX−XXX

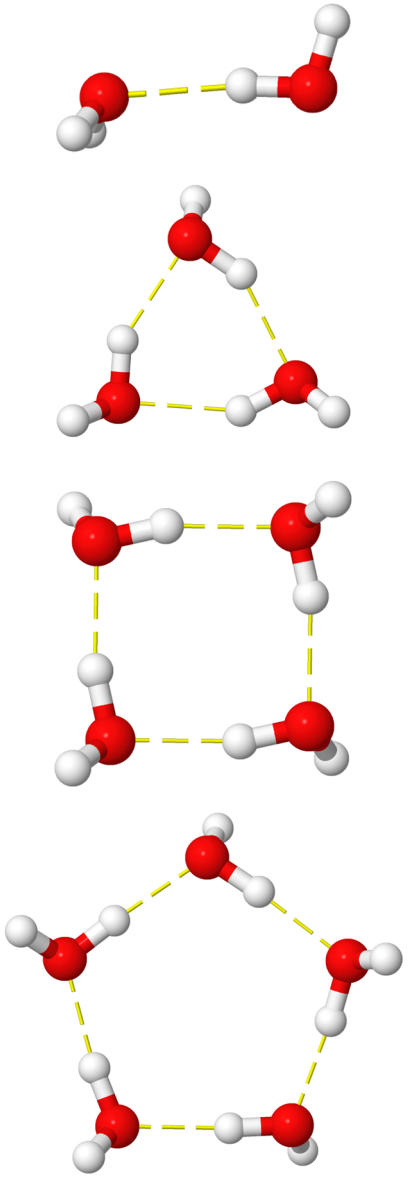

Figure 1. $(H_2O)_n$ minima (n = 2−5) examined in this study.

structural transition for water clusters. Six water molecules form the smallest group for which three-dimensional hydrogen-bonding networks (see Figure 2) possess lower electronic energies than configurations exhibiting the two-dimensional homodromic motif seen in the trimer, tetramer, and pentamer.[26,50,59−63] (Note that "two-dimensional" here refers to a planar or quasi-planar arrangement of the oxygen atoms.)

The first isolated three-dimensional structure characterized experimentally was the "cage" form observed by Liu et al.[64] CCSD(T) CBS limit energies[59] and full-dimensional quantum simulations[65] of low-lying hexamer isomers suggested that the "prism" form has a lower electronic energy and should be nearly isoenergetic with the cage after accounting for zero-point vibrational energy (ZPVE). More recently both the cage and the prism have been observed in broadband rotational spectra.[66] The six-membered analog of the smaller homodromic global minima is the higher-energy "ring" structure in Figure 2, for which IR spectra have been recorded in liquid helium droplets[55,67] and in matrix environments.[57,58,68] Firm assignment of vibrational transitions associated with $(H_2O)_6$ is more

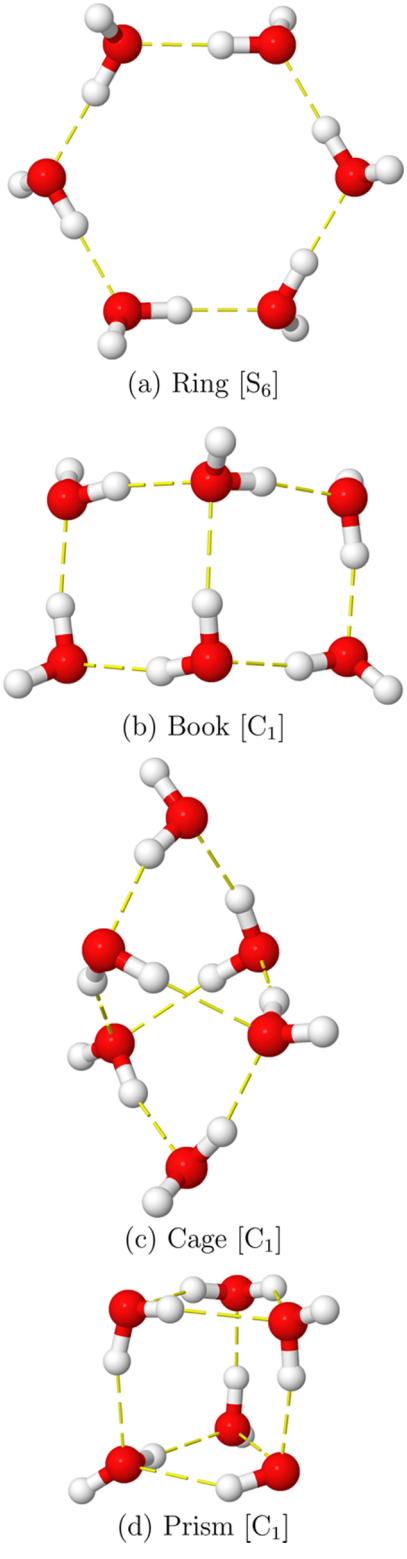

Figure 2. $(H_2O)_6$ minima examined in this study with point group symmetries in square brackets.

challenging not only due to the increased size of the system but also due to the potential presence of multiple isomers.[69−71] Nevertheless, exciting progress continues to be made in the vibrational spectroscopy of water clusters.[53] In fact, the first Raman vibrational spectra of isolated water clusters were reported in 2014.[72]

DOI: 10.1021/acs.jctc.5b00225
J. Chem. Theory Comput. XXXX, XXX, XXX−XXX

While the literature contains a large volume of high-quality ab initio data for water cluster energetics,[8] computed vibrational frequencies of small water clusters at the CCSD(T) level are scarce.[73−77] Bowman and co-workers have made significant theoretical contributions, designing intermolecular ab initio potentials fit to CCSD(T) energies and providing valuable insight into experimental spectra with coupled local mode models which include anharmonicity.[71,73,74,78,79] Another ab initio-based water potential, TTM3-F, has been applied to a range of water clusters from the dimer to the liquid phase.[80]

A reliable description of vibrational frequencies that can be systematically improved and compared to experiment first requires a high-quality harmonic potential. A study of $(HF)_2$ and $(H_2O)_2$ found that anharmonic vibrational frequencies computed with CCSD(T) and a selectively augmented quadruple-ζ basis set yields fundamental frequencies within a few cm^{-1} of experiment for intramonomer modes.[77] In this work, we compute benchmark harmonic vibrational frequency values for the cyclic water trimer, tetramer, and pentamer global minima as well as the ring, book, cage, and prism isomers of the hexamer. In addition to CCSD(T)[81] analytic harmonic frequencies, we use an accurate QM:QM approach[76] based on the many-body expansion[13] to obtain CCSD(T)-quality results analytically with a larger correlation-consistent quadruple-ζ basis set. These current benchmark values are compared to the results of several ab initio methods and two water potentials.

2. THEORETICAL METHODS

Fully optimized geometries and harmonic vibrational frequencies for eight $(H_2O)_m$ (m = 2−6) minima (see Figures 1 and 2) were computed at the MP2 level,[51] employing Dunning's correlation-consistent[82] cc-pVXZ (X = D,T,Q) basis set for hydrogen atoms and aug-cc-pVXZ for the "heavy" atoms (i.e., oxygen). This application of the correlation-consistent family of basis sets, hereafter referred to as haXZ, has been shown to provide dissociation energies and geometries closer to the CBS limit for water clusters than their fully augmented counterparts.[83,84] For each $(H_2O)_m$ isomer, optimal geometries and harmonic vibrational frequencies were also computed with the 2b:Mb CCSD(T):MP2 method (vide infra) and the TTM3-F potential.[80]

All geometry optimizations and harmonic vibrational frequencies were computed with Gaussian09,[85] utilizing analytic gradients and Hessians for the MP2 and CCSD(T):MP2 methods. For the $(H_2O)_5$ and $(H_2O)_6$ clusters, MP2/haQZ vibrational frequencies were computed by finite differences of gradients evaluated with MPQC[86] at displacements generated with PSI4.[87] The CCSD(T) analytic gradients and Hessians needed for the CCSD(T):MP2 calculations were provided by CFOUR.[88] Structures and harmonic frequencies for the TTM3-F potential[80] were computed via finite differences generated and evaluated in Gaussian09 using analytic gradients computed with a freely available copy of the potential.[89] All computations were performed in the "frozen core" approximation (i.e., the 1s-like core electrons of O were not correlated in post-HF calculations). For optimized geometries, the maximum absolute Cartesian force component never exceeds $2.5 \times 10^{-4}\ E_h\ a_0^{-1}$.

To extend the computationally demanding CCSD(T) treatment of electron correlation to larger basis sets, we have applied a QM:QM scheme, based on the traditional many-body expansion for the interaction energy of weakly bound clusters,[13] which we refer to as N-body:Many-body QM:QM.[76,90−96] Here, the many-body expansion is carried out from 1-body (monomer) terms through N-body terms using a high-level QM method, and any higher-order cooperativity in the cluster (>N-body) is captured with a less-demanding QM method. While a reasonable estimate for the energy of a neutral cluster composed of m fragments ($E = E_1 + E_2 + \cdots + E_m$) can sometimes be obtained by truncating the many-body expansion after the inclusion of 2- or 3-body terms (e.g., $E \approx E_1 + E_2 + E_3$),[13,31,93] a much more accurate approximation can be realized by including the trailing terms with a lower-level QM method.[76,93,97−99]

This N-body:Many-body (Nb:Mb) approach applied to a homogeneous or heterogeneous cluster composed of m fragments can be viewed as correcting a many-body expansion truncated at order N by computing all higher-order (N + 1 through m) interactions with a lower level method, as in equation 1.

$$E_{N\mathrm{b:Mb}}^{\mathrm{Hi:Lo}} = \sum_{i=1}^{N} E_i^{\mathrm{Hi}} + \sum_{j=N+1}^{m} E_j^{\mathrm{Lo}} \tag{1}$$

An alternative interpretation of the procedure is as an electron correlation correction, as in equation 2, where the cluster's total supermolecular energy at a lower level of theory (E^{Lo}) is corrected term-by-term with a more complete treatment of electron correlation in a many-body expansion truncated at order N.

$$E_{N\mathrm{b:Mb}}^{\mathrm{Hi:Lo}} = E^{\mathrm{Lo}} + \sum_{i=1}^{N} (E_i^{\mathrm{Hi}} - E_i^{\mathrm{Lo}}) \tag{2}$$

The linear expressions in equations 1 and 2 are easily differentiated to obtain analogous expressions for the gradient and Hessian. Explicit expressions for the geometrical derivatives have already been presented elsewhere.[76,94,96]

This study uses CCSD(T) as the "high-level" method to compute up through the 2-body (2b) terms and MP2 as the "low-level" method to capture all higher-order terms, which defines the 2b:Mb CCSD(T):MP2 method. The 2b:Mb CCSD(T):MP2 technique was applied to the computation of optimized geometries and harmonic vibrational frequencies of $(H_2O)_n$ clusters (n = 3−6).[76] With the haDZ basis set, 2b:Mb CCSD(T):MP2 optimized structures and vibrational frequencies were virtually identical to canonical CCSD(T) results, with a maximum deviation in the harmonic frequencies of <6 cm^{-1} and an average absolute deviation <1 cm^{-1} for all normal modes in a set of 16 different water clusters.[76]

In this work, we extend the 2b:Mb treatment to the larger haTZ and haQZ basis sets. For all minima, 2b:Mb CCSD(T):MP2/haTZ and haQZ optimized geometries and harmonic vibrational frequencies were computed. Since all of the QM:QM computations were performed within the 2-body:Many-body approximation, CCSD(T):MP2 hereafter implies 2b:Mb CCSD(T):MP2.

3. RESULTS AND DISCUSSION

3.1. Water Cluster Geometries. Since the vibrational frequencies of water clusters are sensitive to geometrical changes (particularly for the OH stretching modes),[75] we first briefly discuss the basis set convergence of the CCSD(T):MP2 geometries of in terms of the covalent bond lengths (R(OH)) and the hydrogen bond distances (R(O···H)).

The R(OH) haDZ bond lengths are overestimated by 0.006−0.007 Å relative to corresponding haQZ values for the dimer and trimer. In the larger clusters, the maximum R(OH) deviations are

DOI: 10.1021/acs.jctc.5b00225
J. Chem. Theory Comput. XXXX, XXX, XXX−XXX

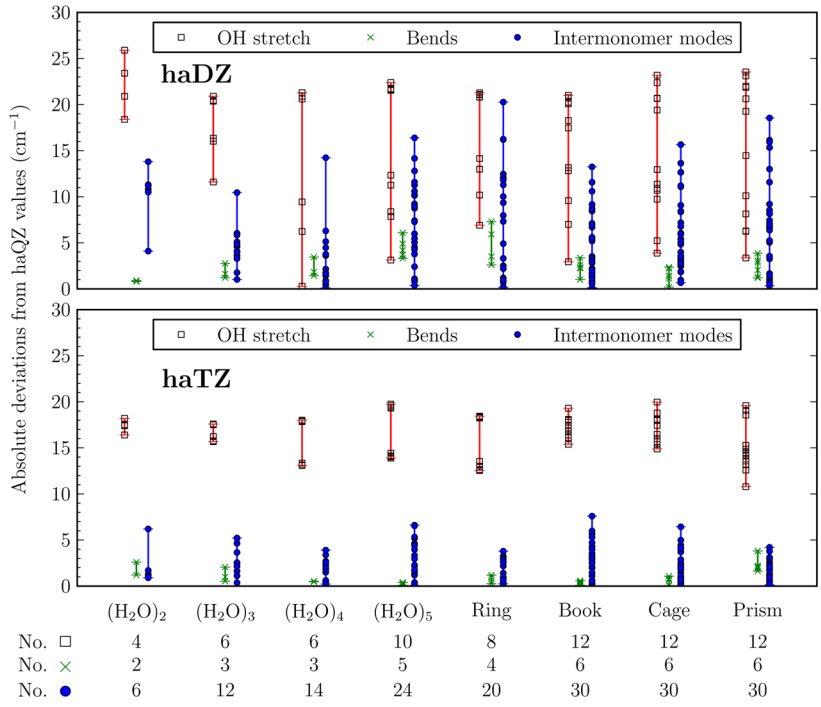

Figure 3. Deviations between 2b:Mb CCSD(T):MP2/haQZ harmonic vibrational frequencies and corresponding haDZ values (top) and haTZ values (bottom). The connecting lines only serve as visual aids. (The number of OH stretches, bends and intermonomer modes is indicated below each isomer.)

very similar, but the deviations cover a much wider range for the clusters with more hydrogen bonds (prism and cage). In most cases, the R(OH) haTZ deviations relative to haQZ are roughly half the magnitude of the corresponding haDZ deviations.

The CCSD(T):MP2/haDZ optimized R(O···H) distances are too long relative to the haQZ values in every case, with the H-bond distances in the dimer and cyclic minima overestimated by 0.01−0.02 Å. The haDZ deviations are larger in the three-dimensional hexamers. Maximum deviations in the prism, cage, and book R(O···H) are 0.07, 0.04, and 0.03 Å. The larger haTZ basis set offers significant improvement in the intermonomer separations, as the largest absolute deviation from the corresponding haQZ reference is only 0.004 Å (cage). The basis set convergence of the R(OH) and R(O···H) parameters can be seen in more detail in Figure S1, Supporting Information.

3.2. Harmonic Vibrational Frequencies. When a particular $(H_2O)_n$ cluster coalesces from n monomers, a total of $6n - 6$ new low-energy vibrational modes are formed (ca. 10−1000 cm^{-1}) that are predominantly of an intermonomer nature. That leaves $3n$ higher-energy intramonomer vibrational modes:n intramonomer bending vibrations (ca. 1600−1800 cm^{-1}) and $2n$ OH stretching vibrations (ca. 3200−3900 cm^{-1}). The changes in the monomer OH stretching frequencies induced by the formation of hydrogen bonds provide valuable spectral signatures for these water clusters. When these small H_2O clusters form, the stretching frequencies of the OH groups participating in the hydrogen bonds (i.e., the "bound OH" stretches or "H-bonded OH" stretches) are shifted to substantially lower energies (on the order of 10^2 cm^{-1}) relative to the OH stretching frequencies of an isolated water monomer (ν_1 = 3657 cm^{-1} and ν_3 = 3756 cm^{-1}).[100] In contrast, the perturbations are much smaller (on the order of a few cm^{-1}) if the OH group is not participating in a hydrogen bond (i.e., the "free OH" stretches). The large shift to lower energies of the bound OH stretches is commonly referred to as a "red shift."

3.2.1. Basis Set Convergence. The accuracy of the CCSD(T):MP2 harmonic frequencies for these clusters was previously demonstrated for the haDZ basis set,[76] where the largest deviations from canonical CCSD(T) typically occurred for the lowest-energy OH stretching mode but never exceeded a few cm^{-1}. In the present study, it was feasible to compute canonical CCSD(T)/haTZ geometries and harmonic frequencies for the $(H_2O)_3$ and $(H_2O)_4$ clusters. The excellent agreement between the canonical CCSD(T) and CCSD(T):MP2 vibrational frequencies clearly extends to the larger haTZ basis set for which the frequencies never differ by more than 1 cm^{-1} for the trimer and 4 cm^{-1} for the tetramer. The average absolute deviation between CCSD(T):MP2/haTZ harmonic frequencies and canonical CCSD(T) results for all of the normal modes in these two clusters is only 0.9 cm^{-1}. (All CCSD(T) and CCSD(T):MP2 unscaled harmonic vibrational frequencies computed with the haTZ basis set are provided in the Supporting Information).

The basis set convergence of the CCSD(T):MP2 harmonic frequencies is consistent with another study[77] that examined the basis set convergence of the MP2 and CCSD(T) harmonic vibrational frequencies for $(H_2O)_2$ and $(HF)_2$. That work demonstrated that basis sets of at least quadruple-ζ quality (with or without counterpoise corrections) are required to obtain MP2 frequencies that are consistently within 10 cm^{-1} of the estimated CBS limit values obtained from basis sets as large as aug-cc-pV6Z.

The absolute deviations of the CCSD(T):MP2/haDZ and haTZ frequencies relative to haQZ are plotted in Figure 3 (all of which are provided in the Supporting Information). For the dimer, the CCSD(T):MP2/frequencies are actually pure CCSD(T) frequencies computed in ref 77. Tabulated below the figure are the number of OH stretches (□ symbols), bending modes (× symbols), and intermonomer modes (○ symbols). The deviations of the harmonic OH stretching frequencies from haQZ values exceed 25 cm^{-1} with the haDZ basis set and

DOI: 10.1021/acs.jctc.5b00225
J. Chem. Theory Comput. XXXX, XXX, XXX−XXX

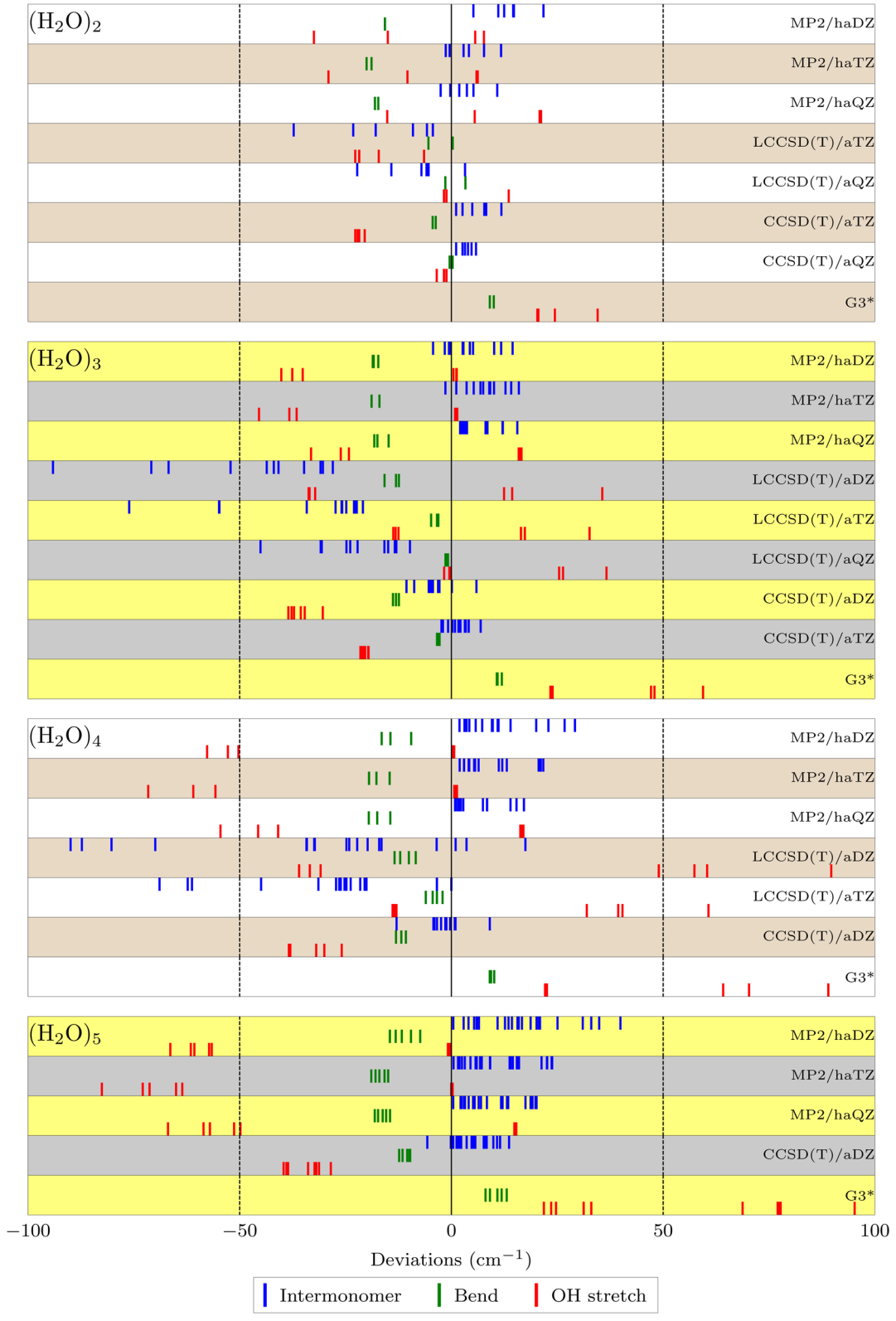

Figure 4. Deviations from the 2b:Mb CCSD(T):MP2/haQZ harmonic vibrational frequencies of $(H_2O)_n$ isomers ($n = 2–5$) for various levels of theory.

approach nearly 20 cm^{-1} with the haTZ basis set. None of the OH stretching frequencies computed with the haTZ basis set lies within 10 cm^{-1} of the haQZ value. The haTZ basis set does offer significant improvement over haDZ for intermonomer frequencies. The maximum deviations in these modes with the haTZ basis set are typically less than half of the magnitude of the corresponding maximum deviations associated with the haDZ basis set.

3.2.2. Performance of Other Electronic Structure Methods. In Figure 4, harmonic vibrational frequencies of $(H_2O)_n$ ($n = 2–5$) clusters computed with MP2, LCCSD(T), and the CCSD(T) methods using double-, triple- and quadruple-ζ basis sets are

DOI: 10.1021/acs.jctc.5b00225
J. Chem. Theory Comput. XXXX, XXX, XXX−XXX

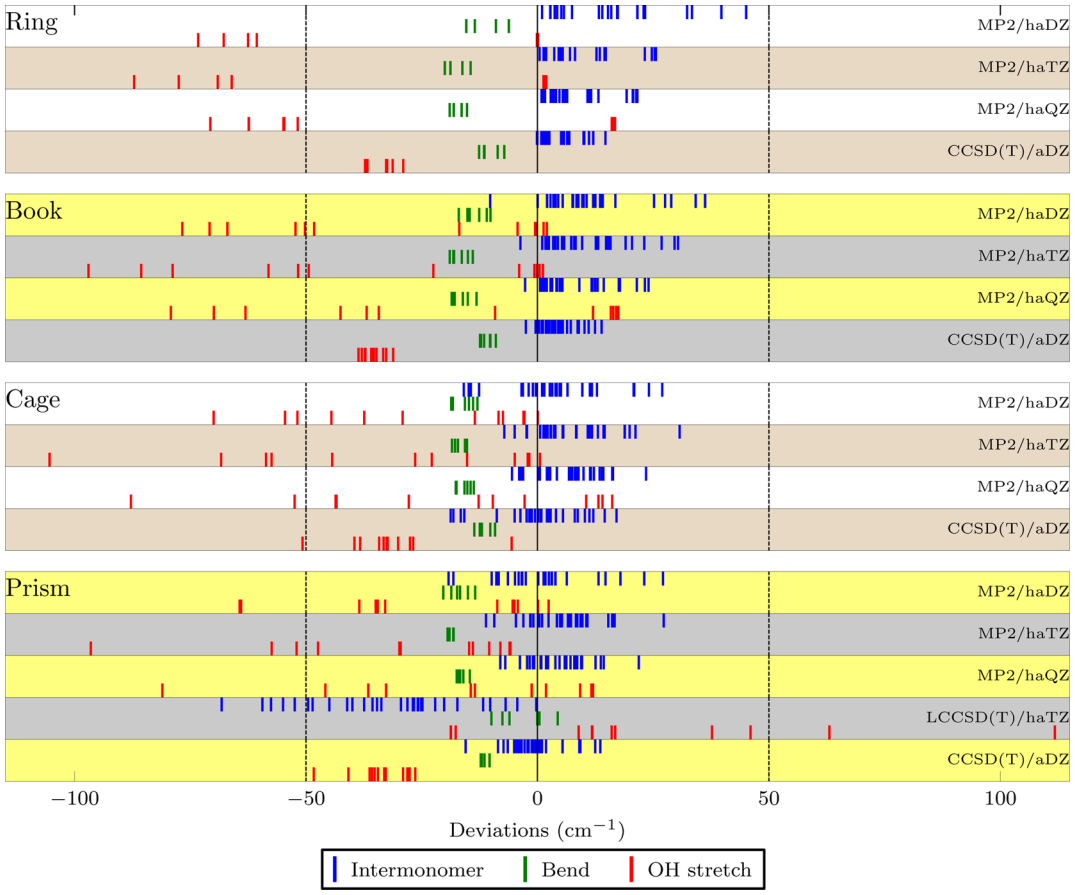

Figure 5. Deviations from the 2b:Mb CCSD(T):MP2/haQZ harmonic vibrational frequencies of $(H_2O)_6$ isomers for various levels of theory.

compared to the benchmark CCSD(T):MP2/haQZ frequencies. The deviations from the reference values are plotted along the *x*-axis as vertical bars, with each bar corresponding to a single harmonic frequency. Each row of Figure 4 presents the results for a particular method and basis set (labeled on the far right) within a particular $(H_2O)_n$ cluster (labeled on the far left). Within each of these rows, the results are further divided into the deviations for intermonomer modes (blue bars on the top of each row), bending modes (green bars in the middle of each row), and OH stretching modes (red bars at the bottom of each row).

For a given cluster in Figure 4, the first three rows give the deviations for MP2/haDZ, MP2/haTZ and MP2/haQZ values, respectively. The largest discrepancies between MP2 and the benchmark CCSD(T):MP2/haQZ frequencies occur for OH stretching frequencies. For example, the very first two rows of red bars in Figure 4 show that MP2/haDZ and MP2/haTZ computations underestimate the OH stretching frequencies by roughly 30 cm^{-1} for the dimer. With the haQZ basis set (third row of red bars), the MP2 stretching frequencies are slightly closer to the reference values, but the largest deviations in this case are due to 2 OH stretches overestimated by ca. 20 cm^{-1}. For the intermonomer modes (blue bars at the top of each row), the MP2 deviations are virtually indistinguishable for the haTZ and haQZ basis sets. The average absolute deviation in the intermonomer modes of $(H_2O)_2$ is <5 cm^{-1} for MP2/haTZ and MP2/haQZ frequencies. The MP2 bending frequencies (green bars in the middle of the each row) are consistently underestimated relative to CCSD(T) by 16−20 cm^{-1} in the dimer.

The MP2 results for $(H_2O)_3$, $(H_2O)_4$, and $(H_2O)_5$ indicate that the deviations from CCSD(T) in the OH stretching frequencies (red bars) increase with cluster size. In particular, the bound OH stretching modes are responsible for the largest discrepancies in clusters larger than the dimer. For these $(H_2O)_n$ clusters, where n = 3−5, previous comparison of CCSD(T) and MP2 harmonic frequencies with the aug-cc-pVDZ basis set has shown that the MP2 method overestimates the red shift of the hydrogen-bonded bound stretching modes.[75] In Figure 4, the n leftmost red bars on each MP2 row correspond to the deviations in bound OH stretching frequencies for a given $(H_2O)_n$ cluster (n > 2). (See Supporting Information for a complete list of harmonic frequencies.) In the trimer, tetramer, and pentamer, the most red-shifted OH stretching frequency is underestimated at the MP2/haQZ level by 33, 55, and 67 cm^{-1}, respectively.

For the intermonomer modes (blue bars), the MP2 deviations increase more slowly with cluster size compared to OH stretching modes (red bars). From the dimer to the pentamer, the MP2/haQZ average absolute deviation only increases from 4 to 9 cm^{-1} (and from 5 to 11 cm^{-1} with haTZ). In stark contrast, however, intermonomer frequencies computed with the haDZ basis set are overestimated relative to the CCSD(T):MP2/haQZ benchmark values by as much as 40 cm^{-1} in $(H_2O)_5$. The accuracy of MP2 water bending frequencies remains consistent with increasing cluster size. Average and maximum absolute deviations in these modes are between 16 and 20 cm^{-1} for $(H_2O)_3$, $(H_2O)_4$ and $(H_2O)_5$ at the MP2/haQZ level.

Figure 5 compares MP2 harmonic frequencies for the hexamer structures to benchmark CCSD(T):MP2/haQZ values and is organized in the same manner as Figure 4. The first four rows of

DOI: 10.1021/acs.jctc.5b00225
J. Chem. Theory Comput. XXXX, XXX, XXX−XXX

Figure 5 give the frequency deviations for the ring hexamer, a cyclic isomer analogous to the global minimum configurations of $(H_2O)_3$, $(H_2O)_4$, and $(H_2O)_5$. The deviations of the MP2 frequencies of the ring are similar to those seen in $(H_2O)_5$. With each of the three basis sets employed in the MP2 calculations, the average absolute deviation across all harmonic frequencies (17−20 cm^{-1}) is only 1 cm^{-1} larger in the $(H_2O)_6$ ring than in the pentamer. The MP2 deviations for each subset of normal modes (intermonomer with blue bars, bend with green bars and OH stretches with red bars) are also very similar between the pentamer and ring structures, with the largest deviations corresponding to underestimated bound stretching frequencies (far left red bars in each row).

The book, cage, and prism hexamers are not homodromic cyclic structures, instead having seven, eight, and nine hydrogen bonds (and bound stretching modes), respectively. Like the cyclic minima, the largest differences between MP2 and CCSD(T) frequencies also occur in the most red-shifted stretching modes. The most red-shifted OH stretching frequencies computed for these three hexamer isomers at the MP2/haQZ level fall 79−88 cm^{-1} lower than the current benchmark reference values. This discrepancy actually exceeds 100 cm^{-1} with the haTZ basis set for the cage isomer. For the bending modes and intermonomer modes, the deviations between CCSD(T):MP2 and MP2 do not significantly increase for the hexamer isomers relative to the cyclic pentamer. With the haQZ basis set, the average absolute deviations for the bending frequencies are 16−17 cm^{-1} and the average absolute deviations for the intermonomer modes range from 7−9 cm^{-1}.

The CCSD(T)/aDZ bound stretching deviations in Figure 5 are interesting because the basis set incompleteness error in these modes is apparently less than the intrinsic error of the MP2 method. For the most red-shifted OH mode in each hexamer, the CCSD(T)/aDZ values are roughly 30−40 cm^{-1} closer to the benchmark reference frequencies than the MP2/haQZ values. In addition, the intermonomer modes calculated at the CCSD(T)/aDZ level are closer to the reference values, with smaller average and maximum absolute deviation values for every hexamer in Figure 5. This is not the case for the free OH stretching modes, as the CCSD(T)/aDZ harmonic frequencies are underestimated by more than 30 cm^{-1} in each $(H_2O)_6$ isomer.

Harmonic vibrational frequencies have also been reported[73] for $(H_2O)_2$, $(H_2O)_3$, $(H_2O)_4$, and the prism isomer of $(H_2O)_6$ that were obtained numerically with a local treatment of electronic correlation at the CCSD(T) level of theory, denoted LCCSD(T). The T0 approximation[101] was employed for the triple excitations in those computations. The deviations between these LCCSD(T) harmonic frequencies and CCSD(T):MP2/haQZ values are also shown in Figures 4 and 5 below the MP2 results. The LCCSD(T) frequencies from ref 73 were computed using fully augmented a*XZ* basis sets. As such, the deviations of available canonical CCSD(T) frequencies computed with a*XZ* basis sets (from refs 73 and75) are also shown in the row(s) following the LCCSD(T) deviations. Together they demonstrate that the largest deviations associated with the LCCSD(T) frequencies are not due to the small differences in the basis set (vide infra).

For the dimer, the OH stretching frequencies computed with the LCCSD(T) method compare favorably with the canonical CCSD(T) results obtained with the same basis set. The maximum LCCSD(T)/aTZ deviation from the reference values is no larger than that for CCSD(T)/aTZ. In fact, the average absolute deviation is actually of smaller magnitude for the former than the latter. The LCCSD(T)/aQZ OH stretches for $(H_2O)_2$ are, on average, within 5 cm^{-1} of the reference benchmark values. However, the largest deviation associated with the LCCSD(T)/aQZ OH stretching modes in the dimer is due to the important bound stretching mode that is too large by more than 13 cm^{-1}. The free stretches at this level of theory are all within 2 cm^{-1} of the CCSD(T)/haQZ values.

The LCCSD(T) frequencies of the trimer and tetramer show much larger deviations relative to the benchmark CCSD(T):MP2/haQZ values. The maximum absolute deviations for LCCSD(T)/aTZ and aQZ frequencies are more than twice what is seen for the same basis sets in $(H_2O)_2$. The LCCSD(T)/aTZ frequencies reported for $(H_2O)_3$ and $(H_2O)_4$ underestimate several intermonomer modes by more than 50 cm^{-1} (blue bars on the far left). The aQZ basis set offers some improvement for these modes in the trimer, but the largest deviation still approaches 50 cm^{-1}. The LCCSD(T) method actually reproduces the canonical CCSD(T) bending frequencies very well when computed with the same basis set, always within 5 cm^{-1} for the clusters in Figure 4.

The only LCCSD(T) values available for these hexamer isomers are the haTZ harmonic frequencies of the prism.[73] These data help show how the LCCSD(T) deviations corresponding to OH stretching modes (red bars) grow as the cluster size increases. The largest deviations from the benchmark CCSD(T):MP2/haQZ stretching frequencies are due to bound OH stretches (red bars to the far right of the LCCSD(T) rows in Figures 4 and 5). The maximum overestimation of these OH stretching frequencies increases from 33 cm^{-1} in the trimer to 61 cm^{-1} in the tetramer with the aTZ basis set and to more than 100 cm^{-1} in the prism with the haTZ basis set. The LCCSD(T)/haTZ deviations in the other modes (green and blue bars) of the prism, however, are comparable to those seen for the smaller water clusters.

For $(H_2O)_n$ (n = 2−5) clusters, intramonomer frequencies computed with a modified version[102] of the Gaussian 3 composite method[103] have also been reported in the literature. The harmonic frequencies computed with this model chemistry, hereafter denoted G3*, reproduce the CCSD(T):MP2/haQZ bending frequencies (green bars) to within ca. 10 cm^{-1} regardless of cluster size. The G3*OH stretching frequencies (red bars), on the other hand, are consistently larger than the reference values, with the error increasing to nearly 100 cm^{-1} for the pentamer. No blue bars are plotted for the G3* method because intermonomer frequencies were not reported.[102]

3.2.3. Comparison of Hydrogen Bond Induced Frequency Shifts. It is important to keep in mind that the deviations reported for the OH stretching frequencies of these water clusters in Figures 4 and 5 (red bars) do not necessarily provide insight into the reliability of red shifts computed with the same method. For example, error cancellation between the computed frequencies for the monomer and cluster could produce an accurate red shift even when a method experiences large deviations for the absolute OH stretching frequencies of a cluster.

The magnitude of the largest red shift has been calculated for each cluster by subtracting the lowest-energy OH stretching frequency from ν_3 of the H_2O monomer computed at the same level of theory. Note that application of the CCSD(T):MP2 scheme to a monomer is simply a canonical CCSD(T) computation. As such, the benchmark CCSD(T):MP2/haQZ red shifts are calculated relative to CCSD(T)/haQZ monomer frequencies. At this level of theory, the magnitude of the largest red shift for each cluster ranges from 190 cm^{-1} for the dimer to

DOI: 10.1021/acs.jctc.5b00225
J. Chem. Theory Comput. XXXX, XXX, XXX−XXX

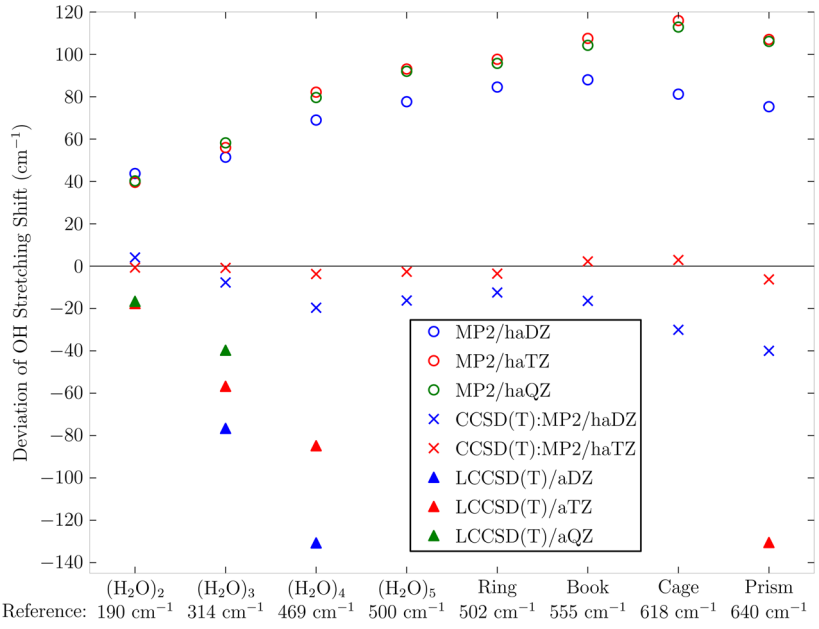

Figure 6. Deviation from the largest 2b:Mb CCSD(T):MP2/haQZ red shift (relative to H_2O ν_3) for various levels of theory.

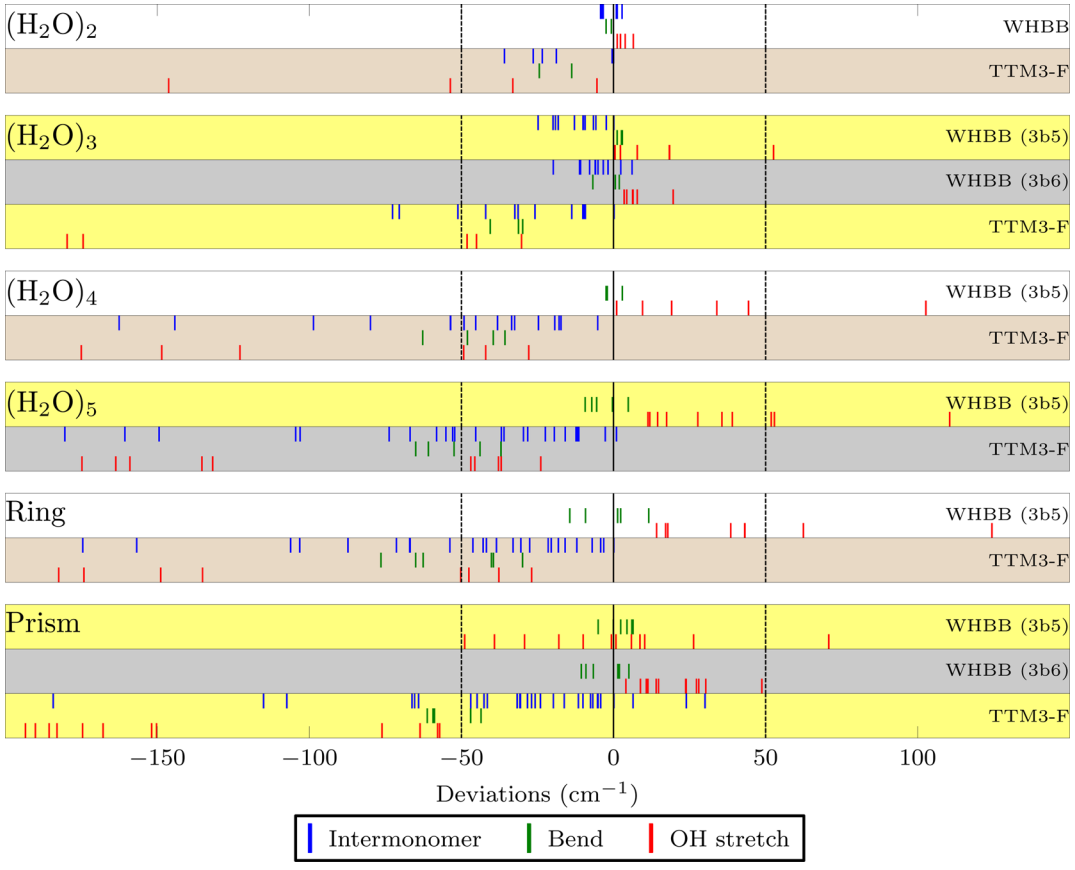

Figure 7. Deviations from the 2b:Mb CCSD(T):MP2/haQZ harmonic vibrational frequencies of select $(H_2O)_n$ isomers (n = 2−6) for WHBB and TTM3-F potentials.

640 cm^{-1} for the prism hexamer. These benchmark values are listed at the bottom of Figure 6, which shows the deviations of other methods from the reference maximum red shifts. The large positive deviations associated with the MP2 method indicate that it consistently overestimates the magnitude of the red shifts in these clusters by roughly 40−120 cm^{-1}. This trend is consistent with the MP2 data presented in Figures 4 and 5 where the bound OH stretching frequencies were appreciably underestimated at the MP2 level of theory (leftmost red bars in the MP2 rows).

In contrast, one sees in Figure 6 that the LCCSD(T) frequencies from ref 73 underestimate the benchmark red shifts. With triple-ζ quality basis sets, the LCCSD(T) deviation

DOI: 10.1021/acs.jctc.5b00225
J. Chem. Theory Comput. XXXX, XXX, XXX−XXX

associated with the largest red shift exceeds 80 cm^{-1} for the tetramer and 130 cm^{-1} for the prism. Again, this trend for the LCCSD(T) data in in Figure 6 is consistent with the sizable overestimation of the OH stretching frequencies seen in Figures 4 and 5 (rightmost red bars in the LCCSD(T) rows). The Supporting Information provides the data needed to calculate every OH frequency shift for each cluster at each level of theory.

Regarding the basis set effects, it is interesting to note that the MP2/haTZ deviations in the bound stretching modes are always larger than the deviations in haDZ or haQZ for clusters larger than the dimer in Figures 4 and 5. Examining the shifts in Figure 6, the haDZ basis set underestimates the red shifts in these clusters, compared with triple-ζ and quadruple-ζ basis sets in each method. Thus, the use of the haDZ basis set slightly compensates for the tendency of MP2 to overestimate the red shifts, producing somewhat smaller deviations than the MP2/haTZ and MP2/haQZ maximum red shifts.

3.2.4. Performance of Water Potentials. The harmonic frequencies computed with two potentials designed by fitting to ab initio data were also included for comparison in Figure 7. The parametrization of the TTM3-F potential[80] is, in part, based on MP2/aDZ frequencies. The WHBB potential[74,78] employs an accurate semiempirical 1-body potential[104] along with fits to CCSD(T)/aTZ energies and MP2/aTZ energies for the 2- and 3-body potentials, respectively. In the WHBB potential, TTM3-F is used for higher-order (beyond 3-body) interactions and long-range interactions. Note that the construction of the WHBB potential is in some ways similar to the 2-body:Many-body CCSD(T):MP2 technique being used to generate our current benchmark values. The WHBB harmonic frequencies used in this comparison were taken from refs 73, 74, and 79.

The WHBB deviations from the benchmark reference harmonic frequencies for $(H_2O)_2$ are quite small. The maximum absolute deviation is <7 cm^{-1}, corresponding to the bound OH stretching mode. The intermonomer frequencies and bending frequencies are within 5 and 3 cm^{-1}, respectively, of the reference data.

In Figure 7, the results include two WHBB variants that are denoted 3b5 and 3b6, which differ in the order of the polynomial expression for the 3-body interaction. Both forms of the WHBB potential give overall good agreement with the CCSD(T):MP2/haQZ frequencies. The largest change between the 3b5 and 3b6 variants is the shift in bound OH stretching frequencies to lower energy, with the 3b6 form decreasing the average absolute deviation from 30 to 10 cm^{-1}.

For larger clusters, the WHBB-3b5 harmonic frequencies overestimate the bound OH stretches. The largest deviation from CCSD(T):MP2 bound stretches occurs in the hexamer ring with one mode overestimated by more than 120 cm^{-1}. This contrasts with the MP2 frequencies for which the largest deviations were associated with the noncyclic hexamers. It should be noted that among these hexamer isomers, the cooperative binding effects (i.e., beyond 2-body interactions) are largest in the cyclic ring.[31] Given the accuracy of this potential for the dimer, the treatment of cooperative effects in WHBB is the most likely source of these large discrepancies.

For the bending modes, the WHBB potential shows excellent agreement with the benchmark values, with a maximum absolute deviation <12 cm^{-1} for the ring isomer. The WHBB intermonomer frequencies are only available for comparison in $(H_2O)_3$, and these are similar to CCSD(T)/aTZ deviations. The TTM3-F vibrational frequencies show much larger deviations. This is not surprising since the potential was parametrized based on MP2/aDZ values. As with the MP2 values, the bound OH stretching frequencies are shifted too low. The largest deviation actually occurs in the $(H_2O)_3$ with the lowest bound stretch predicted over 240 cm^{-1} too low. The TTM3-F deviations for the larger clusters are all <200 cm^{-1}.

4. CONCLUSIONS

The 2b:Mb CCSD(T):MP2 method has been applied to water clusters ranging from $(H_2O)_3$ to $(H_2O)_6$ with basis sets as large as haQZ. Based on results for $(H_2O)_2$ and $(HF)_2$[77] and prior calibration,[76] we expect these harmonic vibrational frequencies to lie close to the CCSD(T) CBS limit. These benchmark-quality harmonic vibrational frequencies served as a reference point to gauge the performance of other harmonic frequencies reported in the literature from other high-level ab initio computations and various water potentials.

MP2 harmonic vibrational frequencies of these water clusters depart significantly from the current benchmark values, particularly for the red-shifted hydrogen-bonded OH stretching modes, where MP2/haQZ computations underestimate the frequencies by more than 80 cm^{-1} and the corresponding red shifts by more than 100 cm^{-1} in the three-dimensional water hexamer structures. CCSD(T) and CCSD(T):MP2 harmonic frequencies computed with modest double-ζ basis sets are in better agreement with benchmark reference values than MP2 frequencies computed with quadruple-ζ basis sets. Compared to the bound OH stretches, MP2 intermonomer, bending and free OH stretching harmonic frequencies computed with the haQZ basis set are in much better agreement with the benchmark values, never differing by more than 25, 20, and 21 cm^{-1} respectively.

For $n \geq 3$, LCCSD(T) harmonic frequencies from the literature deviate substantially from the benchmark values in both intermonomer modes and bound OH stretches due to underestimated red shifts. We plan to investigate how the definition of orbital domains and the degree of electron correlation can be improved to obtain harmonic frequencies in better agreement with canonical CCSD(T) values for these clusters.

The values calculated in this work should guide development and refinement of water potentials. In particular, comparison between CCSD(T)-quality harmonic vibrational frequencies and those from two semiempirical potentials (TTM3-F and WHBB) suggests that the treatment of cooperative effects in water potentials warrants further investigation.

■ ASSOCIATED CONTENT

Ⓢ Supporting Information

Optimized molecular geometries and harmonic vibrational frequencies. This material is available free of charge via the Internet at http://pubs.acs.org.

■ AUTHOR INFORMATION

Corresponding Author

*E-mail: tschumpr@olemiss.edu.

Notes

The authors declare no competing financial interest.

■ ACKNOWLEDGMENTS

This material is based upon work supported by the National Science Foundation under Grant nos. EPS-0903787, CHE-0957317, and CHE-1338056. The authors would also like to

DOI: 10.1021/acs.jctc.5b00225
J. Chem. Theory Comput. XXXX, XXX, XXX−XXX

thank the Mississippi Center for Supercomputing Research for providing computational resources.

REFERENCES

(1) Pimentel, G. C.; McClellan, A. L. *The Hydrogen Bond*; W.H. Freeman: San Francisco, CA, 1960.
(2) Jeffrey, G. A.; Saenger, W. *Hydrogen Bonding in Biological Structures*; Springer-Verlag: Berlin, 1994.
(3) Stone, A. *The Theory of Intermolecular Forces*; Clarendon: Oxford, 1997.
(4) Scheiner, S. *Hydrogen Bonding: A Theoretical Perspective*; Oxford University Press: New York, 1997.
(5) Grabowski, S. J. *Hydrogen Bonding - New Insights, in Challenges and Advances in Computational Chemistry and Physics*; Springer: New York, 2006.
(6) Gilli, G.; Gilli, P. *The Nature of the Hydrogen Bond- IUCr Monographs on Crystallography - 23*; Oxford University Press: New York, 2009.
(7) Keutsch, F. N.; Saykally, R. J. *Proc. Natl. Acad. Sci. U.S.A.* **2001**, *98*, 10533−10540.
(8) Howard, J. C.; Tschumper, G. S. *WIREs Comput. Mol. Sci.* **2014**, *4*, 199−224.
(9) Morokuma, K.; Pedersen, L. *J. Chem. Phys.* **1968**, *48*, 3275−3282.
(10) Kollman, P. A.; Allen, L. C. *J. Chem. Phys.* **1969**, *51*, 3286−3293.
(11) Diercksen, G. H. F. *Chem. Phys. Lett.* **1969**, *4*, 373−375.
(12) Morokuma, K.; Winick, J. R. *J. Chem. Phys.* **1970**, *52*, 1301−1306.
(13) Hankins, D.; Moskowitz, J. W.; Stillinger, F. H. *J. Chem. Phys.* **1970**, *53*, 4544−4554.
(14) Del Bene, J.; Pople, J. *J. Chem. Phys.* **1970**, *52*, 4858−4866.
(15) Diercksen, G. H. F. *Theor. Chim Acta* **1971**, *21*, 335−367.
(16) Del Bene, J. E. *J. Chem. Phys.* **1971**, *55*, 4633−4636.
(17) Popkie, H.; Kistenmacher, H.; Clementi, E. *J. Chem. Phys.* **1973**, *59*, 1325−1336.
(18) Matsuoka, O.; Clementi, E.; Yoshimine, M. *J. Chem. Phys.* **1976**, *64*, 1351−1361.
(19) Tschumper, G. S.; Leininger, M. L.; Hoffman, B. C.; Valeev, E. F.; Schaefer, H. F.; Quack, M. *J. Chem. Phys.* **2002**, *116*, 690−701.
(20) Kalescky, R.; Zou, W.; Kraka, E.; Cremer, D. *Chem. Phys. Lett.* **2012**, *554*, 243−247.
(21) Lane, J. R. *J.Chem. Theory Comput.* **2013**, *9*, 316−323.
(22) Clementi, E.; Kołos, W.; Lie, G.; Ranghino, G. *Int. J. Quantum Chem.* **1980**, *17*, 377−398.
(23) Koeler, J.; Saenger, W.; Lesyng, B. *J. Comput. Chem.* **1987**, *8*, 1090−1098.
(24) Hermansson, K. *J. Chem. Phys.* **1988**, *89*, 2149−2159.
(25) Mó, O.; nez, M. Y.; Elguero, J. *J. Chem. Phys.* **1992**, *97*, 6628−6638.
(26) Mhin, B. J.; Kim, J.; Lee, S.; Lee, J. Y.; Kim, K. S. *J. Chem. Phys.* **1994**, *100*, 4484−4486.
(27) Xantheas, S. S. *J. Chem. Phys.* **1994**, *100*, 7523−7534.
(28) Hodges, M. P.; Stone, A. J.; Xantheas, S. S. *J. Phys. Chem. A* **1997**, *101*, 9163−9168.
(29) Karpfen, A. Case Studies in Cooperativity in Hydrogen-Bonded Clusters and Polymers. In *Molecular Interactions*; Wiley: New York, 1997; pp 265−296.
(30) Masella, M.; Gresh, N.; Flament, J.-P. *J. Chem. Soc., Faraday Trans.* **1998**, *94*, 2745−2753.
(31) Xantheas, S. *Chem. Phys.* **2000**, *258*, 225−231.
(32) Pugliano, N.; Saykally, R. *Science* **1992**, *257*, 1937−1940.
(33) Schütz, M.; Bürgi, T.; Leutwyler, S.; Bürgi, H. B. *J. Chem. Phys.* **1993**, *99*, 5228−5238.
(34) Wales, D. J. *J. Am. Chem. Soc.* **1993**, *115*, 11180−11190.
(35) Liu, K.; Loeser, J.; Elrod, M.; Host, B.; Rzepiela, J.; Pugliano, N.; Saykally, R. *J. Am. Chem. Soc.* **1994**, *116*, 3507−3512.
(36) Schütz, M.; Klopper, W.; Lüthi, H.-P. *J. Chem. Phys.* **1995**, *103*, 6114−6126.
(37) Fowler, J. E.; Schaeffer, H. F., III *J. Am. Chem. Soc.* **1995**, *117*, 446−452.
(38) Wales, D.; Walsh, T. *J. Chem. Phys.* **1996**, *105*, 6957−6971.
(39) Wales, D.; Walsh, T. *J. Chem. Phys.* **1997**, *106*, 7193−7207.
(40) Taketsugu, T.; Wales, D. *Mol. Phys.* **2002**, *100*, 2793−2706.
(41) Anderson, J. A.; Crager, K.; Fedoroff, L.; Tschumper, G. S. *J. Chem. Phys.* **2004**, *121*, 11023−11029.
(42) Pérez, J.; Hadad, C.; Restrepo, A. *Int. J. Quantum Chem.* **2008**, *108*, 1653−1659.
(43) Shields, R. M.; Temelso, B.; Archer, K. A.; Morrell, T. E.; Shields, G. C. *J. Phys. Chem. A* **2010**, *114*, 11725−11737.
(44) Ramírez, F.; Hadad, C.; Guerra, D.; David, J.; Restrepo, A. *Chem. Phys. Lett.* **2011**, *507*, 229−233.
(45) Temelso, B.; Archer, K.; Shields, G. *J. Phys. Chem. A* **2011**, *115*, 12034−12046.
(46) Temelso, B.; Shields, G. C. *J. Chem. Theory Comput.* **2011**, *7*, 2804−2817.
(47) Xantheas, S. S.; Dunning, T. H., Jr. *J. Chem. Phys.* **1993**, *98*, 8037−8040.
(48) Xantheas, S. S.; Dunning, T. H., Jr. *J. Chem. Phys.* **1993**, *99*, 8774−8792.
(49) Yoo, S.; Xantheas, S. Structures, Energetics and Spectroscopic Fingerprints of Water Clusters $n = 2-24$. In *Handbook of Computational Chemistry*; Leszczynski, J., Ed.; Springer: New York, 2012; Vol. *2*, pp 761−792.
(50) Xantheas, S. S.; Burnham, C. J.; Harrison, R. J. *J. Chem. Phys.* **2002**, *116*, 1493−1499.
(51) Cremer, D. *WIREs Comput. Mol. Sci.* **2011**, *1*, 509−530.
(52) Nielsen, I.; Seidl, E.; Janssen, C. *J. Chem. Phys.* **1999**, *110*, 9435−9442.
(53) Huisken, F.; Kaloudis, M.; Kulcke, A. *J. Chem. Phys.* **1996**, *104*, 17−25.
(54) Paul, J.; Collier, C.; Saykally, R.; Scherer, J.; O'keefe, A. *J. Phys. Chem. A* **1997**, *101*, 5211−5214.
(55) Burnham, C. J.; Xantheas, S. S.; Miller, M. A.; Applegate, B. E.; Miller, R. E. *J. Chem. Phys.* **2002**, *117*, 1109−1122.
(56) Slipchenko, M.; Kuyanov, K.; Sartakov, B.; Vilesov, A. *J. Chem. Phys.* **2006**, *124*, 241101.
(57) Hirabayashi, S.; Yamada, K. M. *J. Mol. Struct.* **2006**, *795*, 78−83.
(58) Hirabayashi, S.; Yamada, K. M. *Chem. Phys. Lett.* **2007**, *435*, 74−78.
(59) Bates, D. M.; Tschumper, G. S. *J. Phys. Chem. A* **2009**, *113*, 3555−3559.
(60) Tsai, C.; Jordan, K. *Chem. Phys. Lett.* **1993**, *213*, 181−188.
(61) Kim, K.; Jordan, K. D.; Zwier, T. S. *J. Am. Chem. Soc.* **1994**, *116*, 11568−11569.
(62) Kim, J.; Kim, K. S. *J. Chem. Phys.* **1998**, *109*, 5886−5895.
(63) Olson, R.; Bentz, J.; Kendall, R.; Schmidt, M.; Gordon, M. *J. Chem. Theory Comput.* **2007**, *3*, 1312−1328.
(64) Liu, K.; Brown, M.; Carter, C.; Saykally, R.; Gregory, J.; Clary, D. *Nature* **1996**, *381*, 501−503.
(65) Wang, Y.; Babin, V.; Bowman, J.; Paesani, F. *J. Am. Chem. Soc.* **2012**, *134*, 11116−11119.
(66) Pérez, C.; Muckle, M.; Zaleski, D.; Seifert, N.; Temelso, B.; Shields, G.; Kisiel, Z.; Pate, B. *Science* **2012**, *336*, 897−901.
(67) Nauta, K. *Science* **2000**, *287*, 293−295.
(68) Fajardo, M. E.; Tam, S. *J. Chem. Phys.* **2001**, *115*, 6807−6810.
(69) Diken, E.; Robertson, W.; Johnson, M. *J. Phys. Chem. A* **2004**, *108*, 64−68.
(70) Tainter, C.; Skinner, J. *J. Am. Chem. Soc.* **2012**, *137*, 104304−104316.
(71) Wang, Y.; Bowman, J. M. *J. Phys. Chem. Lett.* **2013**, *4*, 1104−1108.
(72) Otto, K. E.; Xue, Z.; Zielke, P.; Suhm, M. A. *Phys. Chem. Chem. Phys.* **2014**, *16*, 9849−9858.
(73) Wang, Y.; Shepler, B. C.; Braams, B. J.; Bowman, J. M. *J. Chem. Phys.* **2009**, *131*, 054511.
(74) Wang, Y.; Huang, X.; Shepler, B. C.; Braams, B. J.; Bowman, J. M. *J. Chem. Phys.* **2011**, *134*, 94509.
(75) Miliordos, E.; Aprà, E.; Xantheas, S. S. *J. Chem. Phys.* **2013**, *139*, 114302.
(76) Howard, J. C.; Tschumper, G. S. *J. Chem. Phys.* **2013**, *139*, 184113.

DOI: 10.1021/acs.jctc.5b00225
J. Chem. Theory Comput. XXXX, XXX, XXX−XXX

(77) Howard, J. C.; Gray, J. L.; Hardwick, A. J.; Nguyen, L. T.; Tschumper, G. S. *J. Chem. Theory Comput.* **2014**, *10*, 5426−5435.
(78) Wang, Y.; Bowman, J. M. *J. Chem. Phys.* **2011**, *134*, 154510.
(79) Wang, Y.; Bowman, J. M. *J. Chem. Phys.* **2012**, *136*, 144113.
(80) Fanourgakis, G. S.; Xantheas, S. S. *J. Chem. Phys.* **2008**, *128*, 074506.
(81) Raghavachari, K.; Trucks, G. W.; Pople, J. A.; Head-Gordon, M. *Chem. Phys. Lett.* **1989**, *157*, 479−483.
(82) Dunning, T. H., Jr. *J. Chem. Phys.* **1989**, *90*, 1007−1023.
(83) Tschumper, G. S. Reliable Electronic Structure Computations for Weak Non-Covalent Interactions in Clusters. In *Reviews in Computational Chemistry*; Lipkowitz, K. B., Cundari, T. R., Eds.; Wiley-VCH, Inc.: Hoboken, NJ, 2009; Vol. *26*, pp 39−90.
(84) Lane, J. R.; Kjaergaard, H. G. J. *Chem. Phys.* **2009**, *131*, 034307.
(85) Frisch, M. J.; Trucks, G. W.; Schlegel, H. B.; Scuseria, G. E.; Robb, M. A.; Cheeseman, J. R.; Scalmani, G.; Barone, V.; Mennucci, B.; Petersson, G. A.; Nakatsuji, H.; Caricato, M.; Li, X.; Hratchian, H. P.; Izmaylov, A. F.; Bloino, J.; Zheng, G.; Sonnenberg, J. L.; Hada, M.; Ehara, M.; Toyota, K.; Fukuda, R.; Hasegawa, J.; Ishida, M.; Nakajima, T.; Honda, Y.; Kitao, O.; Nakai, H.; Vreven, T.; Montgomery, J. A., Jr.; Peralta, J. E.; Ogliaro, F.; Bearpark, M.; Heyd, J. J.; Brothers, E.; Kudin, K. N.; Staroverov, V. N.; Kobayashi, R.; Normand, J.; Raghavachari, K.; Rendell, A.; Burant, J. C.; Iyengar, S. S.; Tomasi, J.; Cossi, M.; Rega, N.; Millam, J. M.; Klene, M.; Knox, J. E.; Cross, J. B.; Bakken, V.; Adamo, C.; Jaramillo, J.; Gomperts, R.; Stratmann, R. E.; Yazyev, O.; Austin, A. J.; Cammi, R.; Pomelli, C.; Ochterski, J. W.; Martin, R. L.; Morokuma, K.; Zakrzewski, V. G.; Voth, G. A.; Salvador, P.; Dannenberg, J. J.; Dapprich, S.; Daniels, A. D.; Farkas, O.; Foresman, J. B.; Ortiz, J. V.; Cioslowski, J.; Fox, D. J. *Gaussian 09*, Revision D.01 Gaussian, Inc.: Wallingford, CT, 2009.
(86) Janssen, C. L.; Nielsen, I. B.; Leininger, M. L.; Valeev, E. F.; Seidl, E. T. *Massively Parallel Quantum Chemistry Program (MPQC)*, Version 2.3.1 Sandia National Laboratories: Livermore, CA, 2004; http://www.mpqc.org (accessed April 21, 2015).
(87) Turney, J. M.; Simmonett, A. C.; Parrish, R. M.; Hohenstein, E. G.; Evangelista, F. A.; Fermann, J. T.; Mintz, B. J.; Burns, L. A.; Wilke, J. J.; Abrams, M. L.; Russ, N. J.; Leininger, M. L.; Janssen, C. L.; Seidl, E. T.; Allen, W. D.; Schaefer, H. F.; King, R. A.; Valeev, E. F.; Sherrill, C. D.; Crawford, T. D. *Wiley Interdisciplinary Reviews: Computational Molecular Science* **2012**, *2*, 556−565.
(88) Stanton, J. F.; Gauss, J.; Harding, M. E.; Szalay, P. G. with contributions from Auer, A. A.; Bartlett, R. J.; Benedikt, U.; Berger C.; Bernholdt, D. E.; Bomble, Y. J.; Cheng, L.; Christiansen, O.; Heckert, M.; Heun, O.; Huber, C.; Jagau, T.-C.; Jonsson, D.; Jusélius, J.; Klein, K.; Lauderdale, W. J.; Matthews, D. A.; Metzroth, T.; Mück, L. A.; O'Neill, D. P; Price, D. R.; Prochnow, E.; Ruud, K.; Schiffmann, F.; Schwalbach, W.; Stopkowicz, S.; Tajti, A.; Vázquez, J.; Wang, F.; Watts, J. D. and the integral packages MOLECULE (J. Almlöf, J.; Taylor, P. R.) and PROPS(Taylor, P. R.) andABACUS Helgaker, T.; Jensen, Aa.; Jørgensen, P.; Olsen, J.) and ECP routines (Mitin, A. V.; van Wüllen, C.) *Coupled-Cluster Techniques for Computational Chemistry (CFOUR)*. For the current version see http://www.cfour.de.
(89) *TTM3-F* program download link at http://www.pnl.gov/science/ttm3f.asp (accessed January 28, 2015).
(90) Hopkins, B. W.; Tschumper, G. S. *J. Comput. Chem.* **2003**, *24*, 1563−1568.
(91) Hopkins, B. W.; Tschumper, G. S. *Mol. Phys.* **2005**, *103*, 309−315.
(92) Hopkins, B. W.; Tschumper, G. S. *Chem. Phys. Lett.* **2005**, *407*, 362−367.
(93) Tschumper, G. S. *Chem. Phys. Lett.* **2006**, *427*, 185−191.
(94) ElSohly, A. M.; Shaw, C. L.; Guice, M. E.; Smith, B. D.; Tschumper, G. S. *Mol. Phys.* **2007**, *105*, 2777−2782.
(95) Bates, D. M.; Smith, J. R.; Janowski, T.; Tschumper, G. S. *J. Chem. Phys.* **2011**, *135*, 044123.
(96) Bates, D. M.; Smith, J. R.; Tschumper, G. S. *J. Chem. Theory Comput.* **2011**, *7*, 2753−2760.
(97) Klopper, W.; Quack, M.; Suhm, M. *Mol. Phys.* **1998**, *94*, 105−119.
(98) Góra, U.; Podeszwa, R.; Cencek, W.; Szalewicz, K. *J. Chem. Phys.* **2011**, *135*, 224102.
(99) Richard, R.; Herbert, J. *J. Chem. Phys.* **2012**, *137*, 064113.
(100) Herzberg, R. *Molecular Spectra and Molecular Structure Vol III - Electronic Spectra and Electronic Structure of Polyatomic Molecules*; Krieger: Malabar, FL, 1991; p 585.
(101) Schütz, M.; Werner, H.-J. *Chem. Phys. Lett.* **2000**, *318*, 370−378.
(102) Watanabe, Y.; Maeda, S.; Ohno, K. *J. Chem. Phys.* **2008**, *129*, 074315.
(103) Curtiss, L. A.; Raghavachari, K.; Redfern, P. C.; Rassolov, V.; Pople, J. A. *J. Chem. Phys.* **1998**, *109*, 7764−7776.
(104) Partridge, H.; Schwenke, D. W. *J. Chem. Phys.* **1996**, *106*, 4618−4639.

DOI: 10.1021/acs.jctc.5b00225
J. Chem. Theory Comput. XXXX, XXX, XXX−XXX